# De-polarization of on-body channels and polarization diversity at 60 GHz

Nechayev, Yuriy I.; Constantinou, Constantinos C.; Wu, Xianyue; Hall, Peter S.

*DOI:*
10.1109/TAP.2014.2361140



*Document Version*
Publisher's PDF, also known as Version of record

*Citation for published version (Harvard):*
Nechayev, YI, Constantinou, CC, Wu, X & Hall, PS 2014, 'De-polarization of on-body channels and polarization diversity at 60 GHz', *IEEE Transactions on Antennas and Propagation*, vol. 62, no. 12, 6915677, pp. 6519-6523. https://doi.org/10.1109/TAP.2014.2361140

performance of the proposed antenna is improved, thus providing an impedance bandwidth larger than that of a conventional dipole antenna. Stable radiation patterns, similar to those of conventional dipole antenna, have been observed. This proposed antenna can be applied to the notebook or tablet personal computer after fitting the case frame and fine tuning.

## ACKNOWLEDGMENT

Assistance in the form of simulation tools from the National Center for High Performance Computing, Hsinchu, Taiwan is acknowledged. The authors wish to thank Y. Tai, Wistron NeWeb Corporation, Hsinchu, Taiwan, for his assistance in the radiation pattern measurement of the antenna. They are also grateful to D.-H. Hsieh for his assistance in the measurement of the antenna with the system ground plane.

## REFERENCES

[1] Y. W. Chi and K. L. Wong, "Wideband printed dipole antenna for DTV signal reception," *Proc. IEEE*, vol. 40, pp. 1–4, 2007.

[2] Y. W. Chi, K. L. Wong, and S. H. Yeh, "End-fed modified planar dipole antenna for DTV signal reception," *Microw. Opt. Technol. Lett.*, vol. 49, no. 3, pp. 676–680, Mar. 2007.

[3] C. T. Lee and K. L. Wong, "Broadband planar dipole antenna for DTV/GSM operation," *Microw. Opt. Technol. Lett.*, vol. 50, pp. 1900–1905, Jul. 2008.

[4] P. Wu, Z. Kuai, and X. Zhu, "Multiband antennas comprising multiple frame-printed dipoles," *IEEE Trans. Antennas Propag.*, vol. 57, no. 10, pp. 3313–3316, Oct. 2009.

[5] Y. H. Cui, R. L. Li, and P. Wang, "A Novel broadband planar antenna for 2G/3G/LTE base stations," *IEEE Trans. Antennas Propag.*, vol. 61, no. 5, pp. 2767–2774, May 2013.

[6] C. Y. D. Sim, H. Y. Chien, and C. H. Lee, "Dual-/triple-band asymmetric dipole antenna for WLAN operation in laptop computer," *IEEE Trans. Antennas Propag.*, vol. 61, no. 7, pp. 3808–3813, Jul. 2013.

[7] J. Jung, H. Choo, and I. Park, "Design and performance of small electromagnetically coupled monopole antenna for broadband operation," *IET Microw. Antennas Propag.*, vol. 1, no. 2, pp. 536–541, Apr. 2007.

[8] S. Risco, J. Anguera, A. Andújar, A. Pérez, and C. Puente, "Coupled monopole antenna design for multiband handset devices," *Microw. Opt. Technol. Lett.*, vol. 52, no. 10, pp. 359–364, Feb. 2010.

[9] J. S. Hong and M. J. Lancaster, *Microstrip Filters for RF/Microwave Applications*. New York, NY, USA: Wiley, 2001.

[10] J. Anguera, A. Andújar, M.C. Huynh, C. Orlenius, C. Picher, and C. Puente, "Advances in antenna technology for wireless handheld devices," *Int. J. Antennas Propag.*, vol. 2013, 2013 [Online]. Available: http://dx.doi.org/10.1155/2013/838364, Article ID 376531

[11] W. Y. Li, K. L. Wong, and S. W. Su, "Broadband integrated DTV antenna for USB dongle application," *Microw. Opt. Technol. Lett.*, vol. 49, no. 5, pp. 1018–1021, May 2007.

[12] C. K. Hsu and S. J. Chung, "A wideband DVB forked shape monopole antenna with coupling effect for USB dongle application," *IEEE Trans. Antennas Propag.*, vol. 58, no. 9, pp. 3029–3036, Sep. 2010.

[13] D. B. Lin, P. C. Tsai, I. T. Tang, and P. S. Chen, "Spiral and multimode antenna miniaturization for DTV Signal Receptions," *IEEE Antennas Wireless Propag Lett.*, vol. 9, pp. 902–905, 2010.

[14] C. Yang, H. Kim, and C. Jung, "Broad dual-band PIFA using self-complementary structure for DVB-H applications," *IET Electron. Lett.*, vol. 46, no. 21, pp. 1418–1419, Oct. 2010.

# De-Polarization of On-Body Channels and Polarization Diversity at 60 GHz

Yuriy I. Nechayev, Constantinos C. Constantinou, Xianyue Wu, and Peter S. Hall

***Abstract*—Measurements of on-body dynamic propagation channels have been performed at 60 GHz using dual-polarized scalar horn antennas. Comparison of the statistics of the measured signals showed that the choice of polarization (vertical or horizontal) does not affect the path losses significantly, and the relative polarization of the two antennas depends on their placement on the body. In volatile links, such as those from the wrist to other parts of the body, random movements equalize the differences between different polarization configurations. These depolarization effects can be exploited to improve link performance through the use of receive diversity with maximal ratio combining. More advanced multiple-input multiple-output diversity methods are found to produce only marginally better performance compared to receive maximal ratio combining.**

***Index Terms*—Millimeter wave propagation, personal area networks, polarization diversity.**

## I. INTRODUCTION

Wireless communications at the V-band frequencies around 60 GHz promise to provide a number of benefits in wireless body-area network (WBAN) applications. Up to 7 GHz of spectrum is available in this band for unlicensed short-range use in many countries around the world. Thus, data rates of tens of Gb/s can be potentially achieved using advanced encoding methods, such as orthogonal frequency-division multiplexing (OFDM). Two proposed network standards, WiGig (IEEE 802.11ad) [1] and WirelessHD [2], utilize this frequency band achieving data rates of up to 7 Gb/s, and up to 28 Gb/s with spatial multiplexing [3].

Electromagnetic waves in the 60 GHz frequency band are subject to fast attenuation with distance and absorption by oxygen molecules in atmosphere. This helps to reduce interference between neighboring communication networks and also enhances network security and covertness. In [4], it was demonstrated that WBANs using communication links at 60 GHz with omnidirectional monopole antennas are detectable at distances more than 10 times shorter than WBANs operating at 2.45 GHz. This is a particularly attractive property for WBANs worn by military personnel in the battlefield.

Covertness of such WBANs can be improved even further, at the same time increasing the wanted signal levels, if omnidirectional antennas are replaced with high-gain directional antennas. If such an antenna is pointed in a nearly vertical direction, it will be less visible to any ground-based detectors, whilst maintaining strong signal strengths along the human body. The challenges posed by this solution include transmit and receive antenna misalignment and polarization mismatch caused by body movements of the WBAN user. The effect of such movements on the radio channel with monopole antennas was investigated in [5] and measurements of radio channels with horn antennas

Manuscript received January 28, 2014; revised May 23, 2014; accepted September 02, 2014. Date of publication October 02, 2014; date of current version November 25, 2014. This work was supported by the UK EPSRC under Grant EP/I010491/1. *(Corresponding author: C. C. Constantinou.)*

The authors are with the School of Electronic, Electrical and Computer Engineering, University of Birmingham, Edgbaston, Birmingham, B15 2TT, U.K. (e-mail: c.constantinou@bham.ac.uk).

Color versions of one or more of the figures in this communication are available online at http://ieeexplore.ieee.org.

Digital Object Identifier 10.1109/TAP.2014.2361140

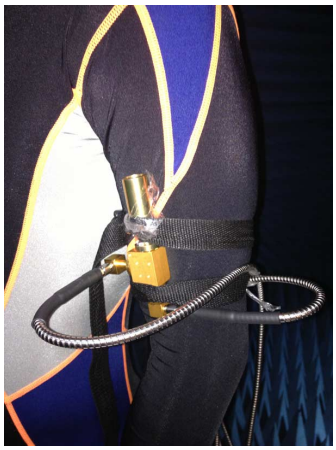

Fig. 1. Scalar horn with an OMT, waveguide-to-coaxial adaptors and coaxial cables, mounted on the arm.

were reported in [6]. Apart from [6] no other work studying polarization diversity for WBANs in the 60 GHz band is known to the authors. There are, however, publications which investigate the effect of polarization in on-body channels at 60 GHz [7] and at lower frequencies [8]–[13].

This communication presents a further and more complete analysis of the measured data presented in [6]. The measurements of on-body radio channels with two dual-polarized scalar horn antennas are presented in Section II. Statistics of the narrowband signal strength and de-polarization effects are given in Sections III and IV, respectively. Then, the effectiveness of polarization diversity in alleviating fading is discussed in Section V, and conclusions are drawn in Section VI.

## II. Measurement Setup

The description of the measurement setup can be found in [6] for radio channels with scalar horns and in [5] for the channels with monopole antennas. It is outlined here briefly for completeness.

The measurements were conducted in an anechoic chamber using a Rohde & Schwarz ZVA67 4-port network analyzer. Two scalar horn antennas were connected to the analyzer through orthomode transducers (OMT) which have two inputs each corresponding to one of two orthogonal polarizations. Thus two orthogonal polarizations were measured simultaneously at the receive antenna, and the transmit antenna switched between its two polarizations within less than 2.1 ms. The antennas were placed on the body as shown in Fig. 1, so that the two measured polarization configurations correspond, respectively, to the electric fields perpendicular (or vertical) and parallel (or horizontal) to the body surface. The four nearly simultaneously measured polarization configurations will be referred to as 'VV', 'VH', 'HV', and 'HH', where 'V' stands for vertical polarization and 'H' for horizontal, and the first letter represents the transmitted polarization state while the second is the received polarization state.

The positions of the antennas on the body define the channels. The measured channels are listed in Table I. In each case, the antennas were oriented in such a way that they were pointing approximately towards each other when the test subject wearing the antennas stood upright looking forward with both arms in the rest position by the sides of the torso. We note that in this pose the polarization of the antenna on the side of the head was at right angles relative to the polarization of the antenna placed on the abdomen or the chest and, therefore, VH and HV configurations are co-polarized in this case and are expected to have stronger signal than VV and HH. 60,001 data points were measured at 60 GHz for each channel and each polarization setup, at the sampling rate of 483 $s^{-1}$, whilst the test subject was performing random sequences of movements resembling various everyday activities. The subject was located inside an anechoic chamber and was wearing a conformal nylon wetsuit in order to eliminate shadowing by loose clothes.

TABLE I
Measurement Sets

| Set Number | Channel | Repetitions |
|---|---|---|
| 1 | head–abdomen | 2 |
| 2 | head–chest | 2 |
| 3 | head–arm | 2 |
| 4 | head–wrist | 1 |
| 5 | arm–wrist | 2 |
| 6 | chest–wrist | 1 |
| 7 | chest–abdomen | 2 |

TABLE II
Median Path Loss

| Meas. Set | VV | VH | HV | HH | Mono |
|---|---|---|---|---|---|
| head–abdomen | 61.0 | 58.2 | 58.1 | 61.4 | NA |
| head–abdomen rpt | 61.7 | 57.9 | 57.3 | 62.6 | NA |
| head–chest | 42.6 | 34.0 | 34.3 | 44.9 | 64.0 |
| head–chest rpt | 46.4 | 38.5 | 38.8 | 49.7 | NA |
| head–arm | 71.7 | 65.0 | 68.0 | 70.4 | 67.0 |
| head–arm rpt | 70.5 | 64.2 | 67.6 | 69.9 | NA |
| head–wrist | >80.0 | >80.0 | >80.0 | >80.0 | 69.2 |
| arm–wrist | 64.8 | 66.7 | 66.4 | 61.6 | 56.8 |
| arm–wrist rpt | 77.3 | >80.0 | 79.5 | >80.0 | NA |
| chest–wrist | >80.0 | >80.0 | >80.0 | >80.0 | 80.7 |
| chest–abdomen | 46.5 | 51.6 | 55.5 | 46.8 | 70.0 |
| chest–abdomen rpt | 46.6 | 50.3 | 53.6 | 46.3 | NA |

NA – data not available

The measurements with omnidirectional quarter-wavelength monopole antennas were performed in a similar manner, as described in detail in [5], but some of the measurement settings were different: 20 001 points were measured per sweep at a sampling rate of 99.7 $s^{-1}$.

All the data were normalized by the back-to-back response of the cables so that the path losses reported below include the antenna losses as well as those due to the environment. The root-mean-squared (RMS) normalized readings corresponding to the measured noise, for the VV, VH, HV, and HH channels of the measurements with the scalar horns, are 86.9, 88.1, 86.9, and 88.1 dB, respectively. The RMS noise value for the monopole measurement was 91.1 dB.

## III. On-Body Channel Statistics

The median path losses measured in each of the four polarization configurations and with the monopole antennas are given in Table II. Similarly, the inter-quartile range (IQR) of the data is presented in Table III. The IQR is the range of path loss values containing 50% of the data (between 25th and 75th percentiles) and quantifies the spread of the path loss around its median. The data in Table II is limited from above by a threshold value of 80 dB, beyond which the effect of thermal noise becomes significant. Some IQR values could not be obtained because the 75th percentile of the path loss also exceeded the 80 dB threshold, and therefore, for such values, only the lower bound of the IQR is given in Table III. For the head-wrist and chest-wrist channels, the 25th percentile also exceeded the threshold, and therefore the IQR could not be determined.

As Tables II and III show, both co-polarized configurations (VV and HH) provide very similar path losses on average. Moreover, the cross-polarized configurations are similar as well. The path loss for the head-chest link is about 10 dB smaller if VH or HV configurations are used, compared to VV and HH. This is because, as was pointed out

TABLE III
PATH LOSS IQR

| Meas. Set | VV | VH | HV | HH | Mono |
|---|---|---|---|---|---|
| head–abdomen | 21.0 | 20.1 | 21.1 | 20.9 | NA |
| head–abdomen rpt | 21.1 | 20.7 | 19.3 | 19.1 | NA |
| head–chest | 13.8 | 13.4 | 12.7 | 13.8 | 16.0 |
| head–chest rpt | 14.9 | 15.6 | 14.4 | 13.6 | NA |
| head–arm | 13.1 | 17.1 | 17.8 | 14.2 | 16.9 |
| head–arm rpt | 15.2 | 17.2 | 16.8 | 15.7 | NA |
| head–wrist | NA | NA | NA | NA | 11.5 |
| arm–wrist | 23.1 | >21.7 | 21.1 | 25.8 | 5.7 |
| arm–wrist rpt | >13.9 | >8.6 | >13.1 | >13.9 | NA |
| chest–wrist | NA | NA | NA | NA | 13.5 |
| chest–abdomen | 6.6 | 7.5 | 7.8 | 8.7 | 8.4 |
| chest–abdomen rpt | 7.4 | 7.6 | 6.5 | 8.7 | NA |

NA – data not available

in Section II, VH and HV are the two co-polarized configurations for this link. On the other hand, for the chest–abdomen link, VV and HH configurations are the co-polarized configurations and, therefore, they have smaller median path losses than the VH and HV configurations. In all the remaining investigated cases the orientation of the antennas relative to each other is changeable, so that all the four polarization configurations produce fairly similar path losses on average. Furthermore, there is no evidence for significant differences in the spread of the path losses among the four polarization configurations, as can be seen from Table III.

Comparing the path losses of the monopole channel and the scalar horn channels, it is noticeable that the horns provide a much stronger signal (at least 10 dB less path loss) than the monopoles in the head–chest and chest–abdomen channels, in which the two antennas of the link do not move relative to each other significantly. However, in the remaining channels in which antenna movements are less restricted, the monopoles can provide a path loss similar to (e.g., the head–arm link case) or even smaller than that of the horns (e.g., the head–wrist and arm–wrist cases, in which the horns point at each other for only a small proportion of the measurement time). Table III shows that the spread of the monopole channel path loss is also similar to that of the horn channels in most cases, except in the case of the arm–wrist link where it is considerably lower. Thus, the choice between an omnidirectional antenna, such as a monopole, and a directive antenna, such as a horn, will depend on the specific communication link. High-gain antennas provide a large benefit in relatively stationary links, while for volatile links beam steering would be required to maintain the link during body movements. On the other hand, omnidirectional antennas provide a noticeable benefit for such links without adding extra complexity.s

## IV. DE-POLARIZATION

The polarizations described in Section II were defined with respect to the body surface orientation at the antenna location. However, as we have already seen, due to the complex geometry of the human body, the antennas with the same polarization defined in this sense are not necessarily co-polarized. Besides, body movements make the antennas rotate relative to each other, thus causing de-polarization of the received signal. Scattering from parts of the body in the local vicinity of the antenna may also cause de-polarization. There are four de-polarization scenarios which can be studied with the available data. They include change of the vertical polarization into a horizontal component at the receive antenna. This effect can be characterized by comparing VV and VH configurations (scenario VV–VH). Vice versa, de-polarization from the horizontal into vertical polarization is characterized by HH and HV configurations (scenario HH–HV). Similarly, because of channel reciprocity, de-polarization at the other (transmit) antenna can

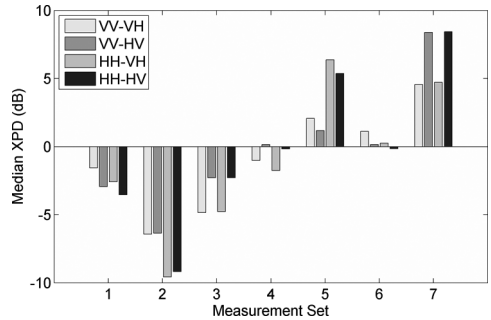


Fig. 2. Median XPD for the measurement sets defined in Table I.

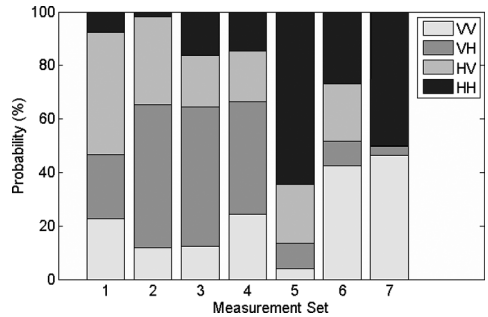


Fig. 3. Probability of a polarization configuration to be dominant for the measurement sets defined in Table I.

also be found in the case of a backward transmission when the propagation direction is reversed. Scenarios VV–HV and HH–VH thus represent de-polarizations in the backward direction of the vertical polarization and horizontal polarization, respectively. The cross-polarization discrimination (XPD) for these four cases is defined here as the ratio of the corresponding co-polarized instantaneous power $P_{VV}$ or $P_{HH}$ to the corresponding cross-polarized instantaneous power $P_{VH}$ or $P_{HV}$, respectively. The median XPDs for each of the seven measured channels is shown in Fig. 2. The negative XPD of the first three links shows that the cross-polarized configurations remain dominant in these links, in which the antennas are mounted at nearly right angles. Similarly, positive XPD for measurement sets 5 and 7, confirms that the antennas remain mostly co-polarized in these links. On the other hand, the two volatile links with one of the nodes on the wrist (measurement sets 4 and 6) are strongly depolarized, with the XPD nearly equal to 0 dB.

Thus, different polarizations of the antennas can be better suited to different channels. Fig. 3 shows the probability of each of the four possible polarizations to produce the strongest signal. For example, the figure shows that for most of the time in the arm–wrist channel the HH polarization configuration is dominant, and for the chest–abdomen channel it is dominant about half of the time, the other half being mostly dominated by the VV configuration. The VV configuration also dominates nearly half of the time in the chest–wrist channel. On the other hand, cross-polarized configurations VH and HV dominated most often in the channels with one of the antennas on the head.

Dominance of the HH configuration in the arm–wrist channel can be explained by the close proximity of the body surface to the propagation path in this case. This leads to the scenario in which not only a single (direct or reflected) path contributes to the received signal but the combined effect of the direct, reflected and surface waves needs to be considered. Norton's solution to the problem of the fields excited by a short dipole above a uniform ground [14] allows for a comparison between the different polarizations in this scenario. Fig. 4 shows the variation with distance of the vertical field component excited by a vertical dipole, $E_z^v$, and of the horizontal component excited by a horizontal dipole, $E_y^h$, above the surface of the human skin with the relative

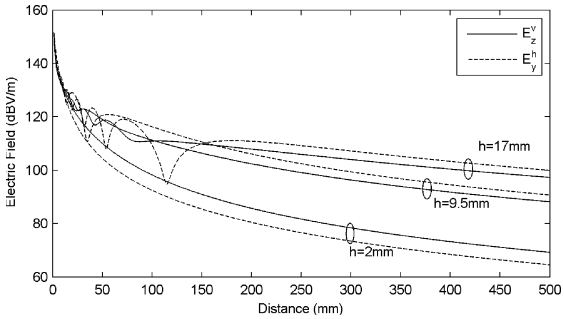


Fig. 4. Theoretical electric fields of the short dipoles above human skin.

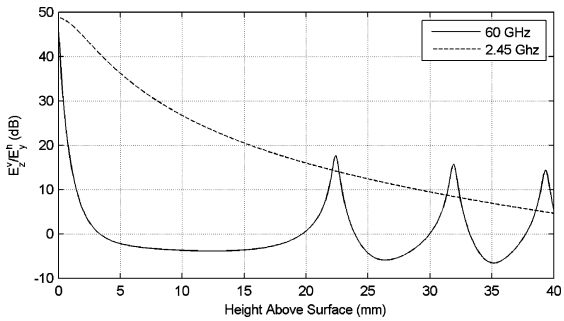


Fig. 5. Ratio of the VV and HH field components at the distance 200 mm.

dielectric constant assumed to be $\varepsilon = 8 - 11j$ [15]. The heights of the field observation point and the dipole are the same. Three heights are shown in Fig. 4 $h = 2$ mm, 9.5 mm, and 17 mm, which correspond to the lowest point of the scalar horn aperture on the arm, its center point, and the top point, respectively. The figure shows that, across most of the distances, the VV configuration dominates over HH only near the surface, at the smaller heights. Fig. 5 shows the ratio of the VV and HH electric fields as a function of height above the surface of the human body. The graph is presented for a separation of 200 mm, which approximately corresponds to the distance between the two horns in the arm–wrist channel. It shows that for antenna heights in the range 3–20 mm, the horizontally polarized antennas should produce stronger signals compared to the vertically polarized ones. This is confirmed by the result presented in Fig. 3 for the arm–wrist channel, where the HH configuration has the probability of occurrence of 64% versus 4% for the VV configuration. This difference was somewhat less in the repeated measurement, but the HH configuration was still dominant with the probability of occurrence 42% compared to 26% for the VV configuration. This is markedly different from lower frequencies, for which VV configuration is known to be dominant [12], [13]. The theoretical curve plotted in Fig. 5 for 2.45 GHz with $\varepsilon = 40 - 11j$, corresponding to dry skin, demonstrates this difference. It should be noted, however, that in general the positions of the antennas relative to the reflecting surfaces and to each other may vary widely in on-body channels. Therefore, as Fig. 3 shows, in the investigated on-body channels, no one configuration remains dominant for more than 60% of the time. Thus the effect of polarization diversity has to be considered in order to maximize the received signal levels. This is the topic of the next section.

## V. Polarization Diversity

Using diversity combining of the four available polarization branches between two transmit and two receive antennas, the effects of the channel depolarization may, in principle, be mitigated. In order to characterize the effectiveness of polarization diversity, we shall use the following definition of the diversity gain (DG). Fig. 6 shows the cumulative distribution functions (CDF) of the four measured signals for the head–abdomen channel. A selection diversity combined signal ("HH-HV combining") is also shown. This is defined as the strongest of the two polarization configurations, HH and HV, thus representing receive diversity combining at the abdomen antenna. We define the diversity gain at the significance level $p$ as the difference between the path gain of the diversity combined signal and that of the strongest of the four original branches at the CDF level $p$. The normal definition would have been to take the difference between the diversity combined signal and the stronger of the two combined branches, but it would ignore the possibility that one of the remaining two channels may provide a better non-diversity link choice. The unconventional definition is intended to assist a 60 GHz WBAN designer to make an informed choice as to whether the added complexity of implementing polarization diversity is worthwhile.

The most straightforward diversity combining method, from a theoretical point of view, would involve selecting the strongest of the four available channels. However, this method would be rather wasteful and impractical since excitation of both transmit ports is required, all four channels need to be directly measured, and only one of them is used. We shall refer to this method as multiple-input multiple-output (MIMO) selection diversity. A switched diversity method, in which the channel is switched according to a specified algorithm every time when the signal falls below a certain threshold, would be more practical. The diversity gain provided by such a method will be bound from above by the diversity gain of MIMO selection combining. A number of practically feasible MIMO and single-input multiple-output (SIMO) combining methods are listed in [16]. The SIMO methods are receive diversity methods, of which we shall consider the selection and maximum ratio combining (MRC) methods. They are simple methods which require a single transmit antenna and very little signal processing. MIMO diversity techniques are more advanced. We estimated the diversity gains for the Alamouti method [16] and for the Tx-selection-Rx-MRC method [16], in which the received signals are combined using the MRC method and the transmitter which provides the strongest combined signal is selected. As was noted in [16], this method outperforms the Alamouti method in terms of diversity gain.

The values of the diversity gain for the measured channels are given in Table IV. The diversity gains were estimated here at levels $p$ of 10% and 25%, because the CDFs at the lower levels were affected by noise in the measurement and could not be reliably estimated. However, it can be expected that the diversity gains at lower levels $p$ should be somewhat higher than those reported in Table IV. The diversity gains were only evaluated for the channels, in which all four branches had a signal-to-noise ratio (SNR) no less than 9 dB at the CDF level $p$. The repeated measurement runs were processed separately and the corresponding diversity gains are also given in Table IV. In most cases the results for the repeated measurements are sufficiently close to each other, thus lending support for the reliability of the measurement procedure.

Table IV shows that, with the exception of head–abdomen channel, SIMO selection diversity produces very little gain. In the case of chest–abdomen channels with the horizontally polarized transmitter, this gain is even negative due to the fact that the vertical transmitter provides a stronger signal than the considered combined signals. As expected, SIMO MRC produces significantly larger diversity gains, which in some cases happen to be similar, or even better than those of the more advanced MIMO combining techniques. This occurs most often when the transmitter of the SIMO channel is vertically polarized. In general, vertical polarization of the transmitter tends to provide higher diversity gains in SIMO MRC. The achieved diversity gain does not exceed 4 dB at $p = 10\%$, and 5 dB at $p = 25\%$. The head–abdomen link benefits most from the use of diversity, whilst the diversity gains for other links are noticeably lower. This is further

TABLE IV
DIVERSITY GAIN (dB)

| Link | SIMO Selection | | | | SIMO MRC | | | | MIMO Selection | MIMO Alamouti | MIMO Tx-Sel-Rx-MRC | |
|---|---|---|---|---|---|---|---|---|---|---|---|---|
| (node1–node2) | V Frwd[a] | H Frwd[a] | V Bkwd[a] | H Bkwd[a] | V Frwd[a] | H Frwd[a] | V Bkwd[a] | H Bkwd[a] | Frwd & Bkwd | Frwd & Bkwd | Frwd | Bkwd |
| | | | | | $p$=10% | | | | | | | |
| head–chest | 1.7 | 1.2 | 2.0 | 0.5 | 3.4 | 2.7 | 3.4 | 2.3 | 2.0 | 3.0 | 3.4 | 3.4 |
| head–chest rpt | 2.3 | 1.2 | 2.5 | 1.1 | 3.8 | 2.4 | 3.7 | 2.5 | 2.7 | 3.2 | 3.8 | 3.7 |
| chest–abdomen | 1.1 | -1.7 | 0.0 | -0.8 | 2.3 | -0.2 | 1.0 | 0.7 | 1.7 | 1.8 | 2.3 | 1.0 |
| chest–abdomen rpt | 1.1 | -1.6 | 0.7 | -0.9 | 2.6 | 0.1 | 2.1 | 0.7 | 2.1 | 2.2 | 2.6 | 2.1 |
| | | | | | $p$=25% | | | | | | | |
| head–abdomen | 3.2 | 3.7 | 3.7 | 3.1 | 4.3 | 4.4 | 4.7 | 3.9 | 4.9 | 4.7 | 4.4 | 4.7 |
| head–abdomen rpt | 3.0 | 3.5 | 4.0 | 2.5 | 3.8 | 4.2 | 4.7 | 3.4 | 4.5 | 4.3 | 4.2 | 4.7 |
| head–chest | 0.2 | 0.3 | 1.1 | 0.1 | 1.8 | 1.2 | 2.1 | 0.9 | 1.5 | 1.7 | 1.8 | 2.1 |
| head–chest rpt | 0.5 | 0.3 | 0.8 | 0.1 | 2.1 | 1.3 | 2.0 | 1.2 | 1.1 | 1.8 | 2.1 | 2.0 |
| head–arm | 1.8 | 1.1 | 0.7 | 2.1 | 3.1 | 2.2 | 2.0 | 3.4 | 3.1 | 3.2 | 3.1 | 3.4 |
| head–arm rpt | 2.5 | 1.4 | 1.4 | 2.5 | 3.7 | 2.7 | 2.6 | 3.6 | 3.7 | 3.7 | 3.7 | 3.6 |
| chest–abdomen | 0.2 | -1.0 | 0.0 | -1.0 | 1.5 | -0.1 | 0.7 | 0.5 | 0.8 | 0.9 | 1.5 | 0.7 |
| chest–abdomen rpt | 0.4 | -0.2 | 0.0 | -0.2 | 1.9 | 1.0 | 1.2 | 1.5 | 0.9 | 1.6 | 1.9 | 1.5 |

[a]Frwd – forward channel (node1 transmits, node2 receives), Bkwd – backward (reversed) channel (node2 transmits, node1 receives)
V, H – polarization of the transmitting node

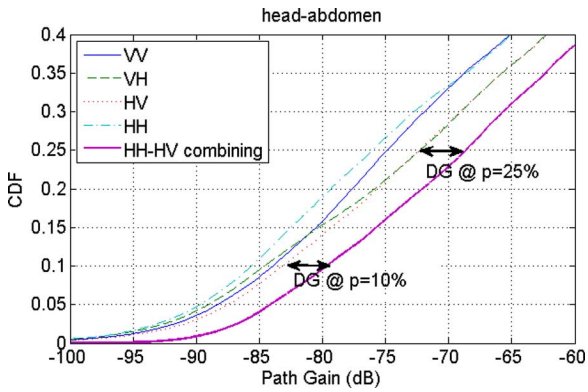


Fig. 6. CDF of the diversity combined signal and definition of diversity gain.

confirmed by the envelope correlation coefficients of the different polarization configurations, which were found to be greater than 0.5 in nearly all the cases. Therefore, diversity has a very limited effect on improving the channel performance when directive antennas are used for transmission. Using the dominant polarization configuration without diversity is a viable option in this case.

## VI. CONCLUSIONS

Analysis of the measurements of dual-polarized on-body propagation channels at 60 GHz demonstrate that when the two antennas are restricted to be close to the body (as is the case in arm–wrist link) the horizontal polarization is likely to be favorable, unlike in the case of lower frequencies, for which vertical polarization is known to be dominant. However, for most channels there is no significant difference in performance between vertically and horizontally polarized high-gain antennas on a human body. The relative orientation of the antennas is important in cases when it does not change very much (such as in head–chest and chest–abdomen links). In most other scenarios, random movements cause depolarization, so that all the polarization configurations yield similar path losses on average. In such a scenario, an omnidirectional monopole antenna is likely to produce lower mean path losses.

Depolarization effects can be mitigated somewhat by diversity methods. Polarization diversity provides diversity gains of up to 5 dB at the level $p = 25\%$. However, in most other cases the achievable gains are smaller, and SIMO selection diversity provides virtually no gain. SIMO MRC, on the other hand, is capable of producing diversity gains on par with the more advanced MIMO diversity techniques.

The final conclusion is that polarization diversity offers little performance advantage in predominantly static 60 GHz WBAN links, whereas SIMO MRC yields in excess of 3 dB diversity gains in predominantly volatile links.

## REFERENCES

[1] Wireless Gigabit Alliance WiGig Alliance, 2012 [Online]. Available: http://www.wigig.org/
[2] WirelessHD, 2012 [Online]. Available: http://www.wirelesshd.org/
[3] WirelessHD Specification Version 1.1 Overview WirelessHD, 2010 [Online]. Available: http://www.wirelesshd.org/pdfs/WirelessHD-Specification-Overview-v1.1May2010.pdf
[4] C. Constantinou *et al.*, "Body-area propagation at 60 GHz," presented at the LAPC 2012, Loughborough, U.K., 2012.
[5] Y. I. Nechayev *et al.*, "Millimetre-wave path-loss variability between two body-mounted monopole antennas," *IET Microw. Antennas Propag.*, vol. 7, pp. 1–7, 2013.
[6] Y. Nechayev *et al.*, "Effect of wearable antenna polarization and directivity on on-body channel path gain at 60 GHz," presented at the AP-S/USNC-URSI, Orlando, FL, USA, 2013.
[7] N. Chahat *et al.*, "On-body propagation at 60 GHz," *IEEE Trans. Antennas Propag.*, vol. 61, pp. 1876–1888, 2013.
[8] L. Akhoondzadeh-Asl *et al.*, "Depolarization in on-body communication channels at 2.45 GHz," *IEEE Trans. Antennas Propag.*, vol. 61, pp. 882–889, 2013.
[9] A. A. Serra *et al.*, "Dual-polarization and dual-pattern planar antenna for diversity in body-centric communications," *IET Microw. Antennas Propag.*, vol. 4, pp. 106–112, 2010.
[10] Y. Yao *et al.*, "Diversity measurements for on-body channels using a tri-polarization antenna at 2.45 GHz," *IEEE Antennas Wireless Propag. Lett.*, vol. 11, pp. 1285–1288, 2012.
[11] Q. H. Abbasi *et al.*, "Experimental investigation of ultra wideband diversity techniques for on-body radio communications," *PIER C*, vol. 34, pp. 165–181, 2013.
[12] T. Uusitupa and T. Aoyagi, "Analysis of dynamic on-body communication channels for various movements and polarization schemes at 2.45 GHz," *IEEE Trans. Antennas Propag.*, vol. 61, pp. 6168–6179, 2013.
[13] S. L. Cotton, R. D'Errico, and C. Oestges, "A review of radio channel models for body centric communications," *Radio Science*, vol. 49, pp. 371–388, 2014.
[14] K. A. Norton, "The propagation of radio waves over the surface of the earth and in the upper atmosphere: Part II," *Proc. IRE*, vol. 25, pp. 1203–1236, 1937.
[15] N. Chahat *et al.*, "Broadband tissue-equivalent phantom for BAN applications at millimeter waves," *IEEE Trans. Microwave Theory Tech.*, vol. 60, pp. 2259–2266, 2012.
[16] S. Catreux *et al.*, "Some results and insights on the performance gains of MIMO systems," *IEEE J. Sel. Areas Commun.*, vol. 21, pp. 839–847, 2003.